Monthly Notices
of the
ROYAL ASTRONOMICAL SOCIETY

MNRAS **445,** 1383–1391 (2014) doi:10.1093/mnras/stu1854

Exomol molecular line lists – VI. A high temperature line list for phosphorus nitride

Leo Yorke,* Sergei N. Yurchenko, Lorenzo Lodi and Jonathan Tennyson

Department of Physics and Astronomy, University College London, Gower Street, WC1E 6BT London, UK

Accepted 2014 September 5. Received 2014 August 29; in original form 2014 July 24

ABSTRACT

Accurate rotational–vibrational line lists for $^{31}P^{14}N$ and $^{31}P^{15}N$ in their ground electronic states are computed. The line lists are produced using an empirical potential energy curve obtained by fitting to the experimental transition frequencies available in the literature in conjunction with an accurate, high-level ab initio dipole moment curve. In these calculations, the programs DPotFit and level 8.0 were used. The new line lists reproduce the experimental wavenumbers with a root-mean-square error of 0.004 cm^{-1}. The line lists cover the frequency range 0–51 000 cm^{-1}, contain almost 700 000 lines each and extend up to a maximum vibrational level of $v = 66$ and a maximum rotational level of $J = 357$. They should be applicable for a large range of temperatures up to, at least, 5000 K. These new line lists are used to simulate spectra for phosphorus nitride at a range of temperatures and are deposited in the Strasbourg data centre. This work is performed as part of the ExoMol project.

Key words: molecular data – opacity – astronomical data bases: miscellaneous – planets and satellites: atmospheres – stars: low-mass.

1 INTRODUCTION

Phosphorus nitride, PN, is a stable, strongly bound, closed shell diatomic molecule. Its electronic ground state has $^1\Sigma^+$ symmetry and its dissociation energy is 51 940 ± 170 cm^{-1} (Gingeric 1969; Cazzoli, Cludi & Puzzarini 2006). It has no low-lying electronically excited states: the lowest excited state is the $^3\Sigma^+$ state at about 25 000 cm^{-1} (for near-equilibrium geometries, ≈1.5 Å), while the lowest lying singlet is the A $^1\Pi$ state at about 40 000 cm^{-1} (Grein & Kapur 1983; de Brouckere, Feller & Koot 1993).

PN is an astrophysically important molecule used to probe different regions of the interstellar medium (ISM). PN was first observed in the ISM by Ziurys (1987), where it was noted that PN was more abundant than originally predicted. It was also observed in the warm star-forming regions Ori (KL), W51M and Sgr B2 by Turner & Bally (1987) as well as in warm molecular clouds of the star-forming regions M17SW and DR 12OH by Turner et al. (1990), suggesting that high-temperature chemistry is important for its formation. PN was detected in the carbon-rich source CRL 2688 by Milam et al. (2008). Most recently, it was observed in the Lynds 1157 B1 shocked region by Yamaguchi et al. (2011) and in the outflow from the protostar IRAS 20386+6751 by Yamaguchi et al. (2012). The chemical mechanism of the PN formation was recently studied by Viana et al. (2009). As yet, PN has not been observed in hotter bodies; however, Visscher, Lodders & Fegley (2006) studied phosphorous and found that in hotter objects, such as brown dwarfs, P-bearing gases such as PN become increasingly important at higher temperatures. Similar results can be expected from exoplanets.

Laboratory spectroscopic studies of PN started with those of Curry, Herzberg & Herzberg (1933a,b). Further experimental investigations were undertaken in the sub-millimetre, radiowave, microwave and infrared frequency ranges (Raymonda & Klemperer 1971; Hoeft, Tiemann & Törring 1972; Wyse, Gordy & Manson 1972; Coquart & Prudhomme 1980; Coquart & Prudhomme 1981; Ghosh, Verma & VanderLinde 1981; Maki & Lovas 1981; Verma, Ghosh & Iqbal 1987; Le Floch et al. 1996; Cazzoli et al. 2006). Some molecular and spectroscopic constants for PN computed ab initio were reported by Raymonda & Klemperer (1971), Wyse et al. (1972), Ghosh et al. (1981), Saraswathy & Krishnamurty (1987) and Ahmad & Hamilton (1995). Several attempts have been made to construct potential energy curves (PECs) of PN (Maki & Lovas 1981; Grein & Kapur 1983; Wong & Radom 1990; McLean, Liu & Chandler 1992; de Brouckere et al. 1993; Kemeny et al. 2003). The vibrationally averaged dipole moments of $^{31}P^{14}N$ for $v = 0$, 1 and 2 were determined by Raymonda & Klemperer (1971) from molecular beam electric resonance measurements.

The aim of this work is to produce accurate rotational–vibrational (ro-vibrational) catalogues of transitions (so-called line lists) for the two stable isotopologues of PN, $^{31}P^{14}N$ and $^{31}P^{15}N$, in their ground electronic states. To this end, an ab initio dipole moment curve (DMC) is used in conjunction with an empirically refined PEC. Our line lists should be complete enough to describe the absorption of PN up to 5000 K. This work is performed as part of the ExoMol project, which aims to provide line lists for all the molecular transitions of importance in the atmospheres of (exo-)planets and cool stars

* E-mail: leo.yorke.10@alumni.ucl.ac.uk

(Tennyson & Yurchenko 2012). The ExoMol methodology has been already applied to a number of diatomic molecules: BeH, MgH, CaH (Yadin et al. 2012), SiO (Barton, Yurchenko & Tennyson 2013), NaCl and KCl (Barton et al. 2014), and AlO (Patrascu, Tennyson & Yurchenko 2014).

2 SOLVING THE NUCLEAR MOTION PROBLEM

A spectroscopic line list comprises transition frequencies (i.e. line positions), Einstein coefficients as well as energies, degeneracies and quantum numbers of the states involved in the transition (Tennyson & Yurchenko 2012). When combined with a partition function, a line list can be used to produce spectra at a given temperature, both in absorption and emission. Each record in the line list corresponds to a transition between two energy levels, in this case ro-vibrational. These levels correspond to characteristic nuclear motions of the molecule, and thus to compute a line list one has to solve the corresponding Schrödinger equation and obtain the energy levels required.

The general form of the radial Schrödinger equation for a diatomic molecule with atoms A and B in a $^1\Sigma^+$ electronic state is given by

$$-\frac{\hbar^2}{2\mu}\frac{\mathrm{d}^2\psi_{v,J}(r)}{\mathrm{d}r^2}+\left[V(r)+\frac{\hbar^2}{2\mu r^2}J(J+1)\right]\psi_{v,J}(r)=E_{v,J}\psi_{v,J}(r), \quad (1)$$

where $V(r)$ is the PEC, $E_{v,J}$ and $\psi_{v,J}$ are, respectively, the bound state eigenvalues and eigenvectors, and μ is the reduced mass given by

$$\mu=\frac{m_A m_B}{m_A+m_B}. \quad (2)$$

In this work, for all nuclear motion calculation we used the following (atomic) masses (Pfeiffer et al. 2012): $m(^{31}\mathrm{P}) = 30.973\,762\,000\,41$ u, $m(^{14}\mathrm{N}) = 14.003\,074\,004\,61$ u and $m(^{15}\mathrm{N}) = 15.000\,108\,898\,18$ u.

Einstein $\mathcal{A}$ coefficients in s^{-1} for ro-vibrational transitions in Σ electronic terms are given by Bernath (2005)

$$\mathcal{A}=\frac{64\pi^4 10^{-36}}{3\,h}\frac{S(J',J'')}{2J'+1}\tilde{\nu}^3\,|\langle\psi_{v',J'}|M(r)|\psi_{v'',J''}\rangle|^2, \quad (3)$$

where J' and J'' are, respectively, the upper and lower rotational angular momentum quantum numbers, $h = 6.626\,069\,57 \times 10^{-27}$ erg s^{-1} is the Planck constant in cgs units, $S(J', J'') = \max(J', J'')$ is the Hönl–London rotational intensity factor, $\tilde{\nu}$ is the transition wavenumber in cm^{-1} and $M(r)$ is the DMC in debyes.

Integrated absorption cross-sections I (also referred to as integrated absorption coefficients or simply as 'line intensities') in cm $\mathrm{molecule}^{-1}$ can be obtained by

$$I=\frac{1}{8\pi c\,\tilde{\nu}^2}\frac{g_{\mathrm{ns}}(2J'+1)}{Q(T)}\mathcal{A}\,\mathrm{e}^{-E''/(k_{\mathrm{B}}T)}\left(1-\mathrm{e}^{-hc\tilde{\nu}/(k_{\mathrm{B}}T)}\right), \quad (4)$$

where $c = 2.997\,924\,58 \times 10^{10}$ cm s^{-1} is the speed of light in cgs units, E'' is the lower state energy, k_{B} is the Boltzmann constant, T is the temperature, $Q(T)$ is the partition functions and g_{ns} is a nuclear spin factor.

To solve the radial Schrödinger equation (1) and compute the energy levels, spectroscopic constants and Einstein coefficients required, we make use of the program LEVEL 8.0 (Le Roy 2007). The PEC and DMC are two prerequisites for these calculations and can be obtained from first principles by solving the Schrödinger equation for the motion of the electrons. Since ab initio PECs are not usually capable of providing accuracies better than a few cm^{-1}, they are commonly refined by fitting to experimental energies or transition frequencies, subject to availability. Conversely, the accuracy of ab initio DMC can be high enough to be competitive with, or even better than, experiment (Lynas-Gray, Miller & Tennyson 1995; Lodi, Tennyson & Polyansky 2011; Tennyson 2014). We use the DPotFit program (Le Roy 2006) to empirically refine the ab initio PEC by fitting to experimental frequencies collected from different literature sources, see Table 1.

3 POTENTIAL ENERGY CURVE

We produced in this work three potential curves for PN: an ab initio one named PEC-A; a semi-empirical one named PEC-S which modifies the ab initio PEC with a single, physically motivated, empirical parameter; and, finally, an empirical PEC-R obtained by fitting the available experimental data. The three PECs are discussed in the following sections.

3.1 The *ab initio* PEC-A

We computed PECs using the well-known CCSD (coupled cluster single and double excitations) and CCSD(T) (coupled cluster single, double and perturbative triple excitations) methods (Bartlett & Musiał 2007) as well as with CASSCF (complete active space self-consistent field), MRCI (internally contracted multi-reference configuration interaction) and MRCI+Q (MRCI with renormalized Davidson correction; Szalay et al. 2012); the +Q correction was computed using the so-called fixed reference function, see Szalay et al. (2012) and the MOLPRO manual for an explanation. CASSCF and MRCI calculations used the full valence reference space and all electrons apart from the phosphorus 1s were correlated. We used correlation-consistent basis sets of the Dunning family (Dunning 1989; Woon & Dunning 1995; Peterson & Dunning 2002) and in particular aug-cc-pwCV5Z and aug-cc-pC6Z, for which we use the shorthand notation awc5z and ac6z. We extrapolated the energies using the formula $E_n = E_\infty + A(n+\frac{1}{2})^{-4}$, which is known to perform very well (Feller & Peterson 2013). A relativistic correction curve was computed as expectation value of the mass–velocity one-electron Darwin operator (MVD1) with the MRCI/ac6z electronic wavefunction and was always included in the calculations. Energies were computed from $r = 2.10\,a_0$ to $6.10\,a_0$ (1.11 to 3.23 Å) in steps of $0.05\,a_0$ and from $r = 6.5\,a_0$ to $16\,a_0$ in steps of $0.5\,a_0$ using MOLPRO (Werner et al. 2012). Calculation of one MRCI energy in the largest ac6z basis set took about 25 GB of disc and 3.5 h on a single CPU.

Some indicative results are reported in Table 2. From these it is clear that errors in ab initio energy levels are very large. Let us first discuss the results in the awc5z basis set. CCSD performs by far the poorest of the methods considered; the (T) correction reduces CCSD errors by a factor of about 6, but the errors are still very large. This seems to indicate that at the very least, CCSDTQ (coupled cluster with full triple and quadruple excitations) should be used for sub-cm^{-1} accuracy, which is computationally unfeasible. CASSCF energy levels are slightly worse than CCSD(T) ones. MRCI energy levels are slightly better than CCSD(T) ones, with errors reduced by a factor of 1.1 or so. Finally, MRCI+Q improves considerably upon MRCI, reducing errors by a factor of about 3. They are still, however, considerably off, with absolute errors in

Table 1. Summary of experimental spectroscopic data available for PN used in our fits.

Reference	Isotopes considered	max v	max J	Wavenumber range cm^{-1}	Number of lines
Cazzoli et al. (2006)	^{31}P ^{14}N	0	17	3.1–26.6	24
Cazzoli et al. (2006)	^{31}P ^{15}N	0	15	3.0–20.9	9
Maki & Lovas (1981)	^{31}P ^{14}N	4, $\Delta v = 1$	53	1217.22–1318.60	22
Wyse et al. (1972)	^{31}P ^{14}N	4, $\Delta v = 0$	8	3.1–12.5	19
Ahmad & Hamilton (1995)	^{31}P ^{14}N	1, $\Delta v = 1$	33	1273.30–1368.49	62
Ghosh et al. (1981)[a]	^{31}P ^{14}N	11	0	1323.17–13 786.95[b]	11

Note: [a]Vibrational band centres derived from the high-resolution study of $^1\Pi$–$^1\Sigma^+$ transition.
[b]Range for the lower ($^1\Sigma^+$) state term values (Ghosh et al. 1981).

Table 2. Vibrational ($J = 0$) energy term values obtained with different electronic structure methods and basis sets. The second column, labelled 'obs.', reports experimental (observed) values from Ahmad & Hamilton (1995) and Irikura (2007), other columns show observed minus calculated. The stated uncertainty of experimental levels is 0.001 cm^{-1} for $v = 0$–4 and 0.05 cm^{-1} for $v = 5$–11. The energy curve corresponding to the results in the last column is referred to as PEC-A in the text. In all cases, a relativistic correction curve computed with the MVD1 Hamiltonian at the MRCI/aug-cc-pV6Z level was included. See Section 3.1 for detailed explanations. All values are in cm^{-1}.

v	obs.	obs. − calc.						
		awc5z CCSD	awc5z CCSD(T)	awc5z CASSCF	awc5z MRCI	awc5z MRCI+Q	ac6z MRCI+Q	ac[56]z MRCI+Q
0	666.79	−40.28	−6.10	9.72	−5.85	−1.77	−2.55	−3.37
1	1989.94	−122.06	−18.78	28.93	−17.67	−5.37	−7.70	−10.16
2	3299.24	−205.74	−32.15	47.80	−29.71	−9.07	−12.97	−17.07
3	4594.64	−291.40	−46.24	66.34	−41.97	−12.88	−18.35	−24.09
4	5876.14	−379.07	−61.11	84.57	−54.44	−16.80	−23.84	−31.24
5	7143.83	−468.69	−76.61	102.66	−66.98	−20.68	−29.31	−38.38
6	8397.42	−560.59	−93.07	120.35	−79.86	−24.79	−35.02	−45.77
7	9637.02	−654.68	−110.35	137.83	−92.93	−28.97	−40.82	−53.27
8	10 862.51	−751.11	−128.59	155.04	−106.26	−33.31	−46.79	−60.96
9	12 073.43	−850.38	−148.20	171.60	−120.27	−38.22	−53.36	−69.26
10	13 270.68	−951.60	−168.27	188.49	−134.00	−42.74	−59.56	−77.22
11	14 453.74	−1055.34	−189.33	205.30	−147.92	−47.35	−65.86	−85.31

cm^{-1} progressively increasing with the vibrational quantum number as about $4.15 \times (v + 1/2)$.

Note that all methods, apart from CASSCF (which anyway is not expected to produce quantitative accuracy), produce energy levels which are too high, suggesting that the outer wall of the potential curve is rising too steeply. Increasing the basis set to ac6z leads to higher energy levels and therefore to even larger errors; basis set extrapolation inevitably leads to errors which are larger still.

We estimate the residual basis set incompleteness error in extrapolated ac[56]z energy levels as half of the difference between ac[56]z and unextrapolated ac6z value; this estimate is well approximated by the expression $0.84 \times (v + 1/2)$, indicating that residual basis set errors are about five times smaller than the observed errors. The relativistic MVD1 correction curve (included in all calculations reported in Table 2) improves agreement with experiment; its effect on vibrational energy levels $v = 0$–11 can be expressed to within 0.04 cm^{-1} by $-1.38 \times (v + 1/2)$. Further, corrections not considered in this work such as higher relativistic effects due to Gaunt, Breit or quantum electrodynamics corrections, as well as adiabatic and non-adiabatic effects, are certainly considerably smaller than the included MVD1 curve, and therefore their inclusion at this stage would not lead to an improvement of the observed residuals. We reach therefore the conclusion that the observed large errors in our best ab initio results are mostly due to incomplete treatment of electron correlation at the CCSD(T) or MRCI+Q level.

Our highest level ab initio PEC is the MRCI+Q/ac[56]z/MVD1, based on extrapolation of the awc5z and ac6z basis sets. The latter PEC will be referred to as PEC-A and leads to a potential well depth $D_e = 51\,605$ cm^{-1}, which is lower by 335 cm^{-1} than the (rather inaccurate) experimental value $51\,940 \pm 170$ cm^{-1}.

It is worth noting that, almost certainly because of partial cancellation of errors, best agreement with experiment is obtained ab initio with the MRCI+Q/acw5z/MVD1 PEC, at least for the range characterized by the available $v = 0$–11 experimental data, which are sensitive to the PEC in the range $r \approx 1.28$–1.80 Å.

3.2 The semi-empirical PEC-S

We considered a simple one-parameter semi-empirical modification of PEC-A as a way of improving its quality in a physically motivated way and with a view to provide a reasonable behaviour in the high-energy range, experimentally unexplored. In particular, we investigated simple scalings of the Davidson correction contribution to the energies. The ab initio MRCI+Q energies can be broken down into a sum of three contributions: $E_{\mathrm{MRCI+Q}} = E_{\mathrm{CASSCF}} + E_{\mathrm{corr}} + E_{+\mathrm{Q}}$, where E_{CASSCF} is the energy of the reference CASSCF wavefunction, $E_{\mathrm{corr}} = E_{\mathrm{MRCI}} - E_{\mathrm{CASSCF}}$ is the MRCI correlation energy and $E_{+\mathrm{Q}}$ is the renormalized Davidson correction, which is given by $E_{+\mathrm{Q}} = E_{\mathrm{corr}}(1 - c_0^2)/c_0^2$, where c_0 is the expansion coefficient of the CASSCF wavefunction in the MRCI one (Szalay et al. 2012).

Table 3. Differences between experimental ('obs.') ro-vibrational energy levels and calculated ones ('calc.') for three PECs $X(r)$, $X = A$, S or R. PEC-A is an ab initio curve based on MRCI+Q/ac[56]z/MVD1; PEC-S is a one-parameter modification of PEC-A; PEC-R is an eight-parameter empirical curve defined by equation (5) and Table 4. Experimental energy levels are computed using the spectroscopic parameters by Ahmad & Hamilton (1995) and include the zero-point energy by Irikura (2007).

v	obs.	obs. − calc.			obs.	obs. − calc.			obs.	obs. − calc.		
		A	S	R		A	S	R		A	S	R
		$J = 0$				$J = 10$				$J = 20$		
0	666.79	− 3.37	0.02	0.00	752.99	− 3.53	0.03	0.00	995.76	− 3.99	0.04	0.00
1	1989.94	− 10.16	0.07	0.00	2075.53	− 10.33	0.08	0.00	2316.58	− 10.80	0.09	0.00
2	3299.24	− 17.07	0.10	0.01	3384.21	− 17.24	0.11	0.00	3623.54	− 17.72	0.12	0.00
3	4594.64	− 24.09	0.10	0.00	4679.00	− 24.27	0.10	0.00	4916.60	− 24.76	0.12	0.00
4	5876.14	− 31.24	0.06	− 0.01	5959.88	− 31.42	0.06	− 0.01	6195.74	− 31.93	0.08	0.00
5	7143.83	− 38.38	0.13	0.14	7226.93	− 38.58	0.12	0.12	7461.00	− 39.16	0.07	0.07
6	8397.42	− 45.77	0.04	0.18	8479.94	− 45.94	0.06	0.20	8712.36	− 46.43	0.12	0.27
7	9637.02	− 53.27	− 0.07	0.28	9718.90	− 53.47	− 0.08	0.28	9949.49	− 54.04	− 0.09	0.28
8	10 862.51	− 60.96	− 0.29	0.38	10 943.77	− 61.16	− 0.28	0.39	11 172.63	− 61.71	− 0.27	0.43
9	12 073.43	− 69.26	− 1.02	0.08	12 154.06	− 69.47	− 1.02	0.09	12 381.12	− 70.07	− 1.04	0.12
10	13 270.68	− 77.22	− 1.33	0.36	13 350.08	− 78.03	− 1.93	− 0.22	13 573.70	− 80.31	− 3.61	− 1.84
11	14 453.74	− 85.31	− 1.68	0.77	14 533.22	− 85.41	− 1.56	0.92	14 757.10	− 85.66	− 1.21	1.35

The Davidson correction tries to approximate the effect of quadruple excitations neglected in the MRCI calculation; in our calculation, the c_0 expansion coefficient as a function of r has the value 0.966 for the near-equilibrium geometry $r = 1.50$ Å, then decreases linearly up to about $r = 2.0$ Å, assumes a minimum value 0.963 at $r = 2.30$ Å and then slowly grows up to a dissociation value of 0.965. The small variation of c_0 with geometry and the fact $c_0 \approx 1$ show that the CASSCF wavefunction is indeed a good reference function for all geometries. By contrast, the expansion coefficient of the Hartree–Fock reference in the MRCI expansions is 0.91 at $r = 1.50$ Å, and then decreases monotonically, is 0.5 at $r = 2.56$ Å and has an asymptotic value of about 0.28. Eventually, we chose a simple direct scaling of the Davidson correction part of PEC-A by a factor of $\alpha = 1.835$. The optimal value of α was found by fitting the experimental $J = 0$ vibrational levels for $v = 0$–11 reported in Table 2. Equivalently, PEC-S can be written as $V_S(r) = V_A(r) + 0.835\, E_{+Q}(r)$, where $V_A(r)$ refers to PEC-A.

This one-parameter semi-empirical PEC, referred to as PEC-S below, reduces very considerably the residuals with experiment of PEC-A and leads to agreement of better than 0.30 cm^{-1} for $v = 0$–8, while last three levels $v = 9$–11 show larger residuals of the order of 1.5 cm^{-1}, see Table 3. The PEC-S leads to a potential well depth $D_e = 51\,742$ cm^{-1}, which is lower by 198 cm^{-1} but compatible with the experimental value, 51 940 ± 170 cm^{-1}. PEC-S was used as the starting point for our subsequent empirical fit.

3.3 The empirical PEC-R

We considered a fully empirical potential energy function based on the extended Morse oscillator function (Šurkus, Rakauskas & Bolotin 1984; Le Roy 2007) as given by

$$V(r) = D_e[1 - e^{-\beta(r)(r-r_e)}]^2,$$

$$\text{where} \quad \beta(r) = \sum_{i=0}^{N_\beta} \beta_i \left(\frac{r^p - r_e^p}{r^p + r_e^p}\right)^i. \qquad (5)$$

The parameters to be fitted are the equilibrium distance r_e, the potential well depth D_e, the coefficients β_i and, finally, the exponent p. Note that one should constrain $p > 0$, $\sum_i \beta_i > 0$ in order to ensure $V(+\infty) = D_e$. In our fits, we truncated the expansion of $\beta(r)$ to three terms ($N_\beta = 2$) for $r < r_e$.

We used DPotFit (Le Roy 2006) to refine the expansion parameters by fitting to the experimental frequencies summarized in Table 1. The main part of the experimental data set includes pure rotational transitions recorded by Cazzoli et al. (2006) and infrared transitions from Ahmad & Hamilton (1995) which cover $v \leq 4$. In order to improve the sampling for higher vibrational excitations, we found it important to include the experimentally derived vibrational energies reported by Ghosh et al. (1981), although with fitting weights smaller by a factor of about 10 than the rest of the data. Since DPotFit is not able to fit to energies directly, we used these energies to generate pseudo-transition frequencies, which allowed us to use data from higher vibrational states, up to $v = 11$, and obtain a much more reasonable fit at the higher energy part of the PEC.

The values for the equilibrium distance r_e and dissociation energy D_e were fixed to the experimentally derived values of Gingeric (1969) and Cazzoli et al. (2006). After some experimentation, the exponent p in equation (5) was set to 4, which allowed us to obtain an accurate fit to the higher energy levels. Four expansion variables β_i were used in the final results. Initial values for the parameters β_i were set to those obtained for the scaled PEC-S. It should be noted, however, that the final results are not very sensitive to the initial ab initio curve (Barton et al. 2013). The final empirical parameters are given in Table 4.

We did not consider explicitly non-adiabatic corrections as these effects are expected to have a small effect (<0.05 cm^{-1}) on most transition frequencies because of the relatively large nuclear masses of PN and the absence of low-lying excited electronic states.

Table 3 gives residuals for a selection of energy levels. These results show that PEC-R generally improves on PEC-S in terms of agreement with experiment and all levels are reproduced to better than 1 cm^{-1}. Table 5 gives residuals for very accurate pure rotational transitions in the microwave region for ^{31}P^{14}N and ^{31}P^{15}N. The ^{31}P^{15}N microwave data in this table are the only available experimental data for this isotopologue. Because of cancellation of errors, calculated rotational transition frequencies for rotational transitions are much more accurate than those for ro-vibrational ones. The ab initio PEC-A gives the worse results, with a root-mean-square (rms) error of 0.03 cm^{-1}; PEC-S improves very considerably over PEC-A and gives an rms error of 0.001 cm^{-1}. Finally, the empirical PEC-R gives the smallest rms of 7×10^{-5} cm^{-1}.

Table 4. Parameters defining the empirical potential surface PEC-R: expansion coefficients β_i, dissociation energy D_e in cm^{-1}, equilibrium bond length r_e in Åand parameter p, see equation (5). For $r < r_e$, the coefficients $\beta(3)$ and $\beta(4)$ are set to zero.

Parameter	Value
D_e/cm^{-1}	51 940
r_e/Å	1.490 869 6082
$\beta(0)$	2.218 524 8572
$\beta(1)$	0.177 496 755 48
$\beta(2)$	0.169 622 361 12
$\beta(3)$	0.142 421 403 68
$\beta(4)$	0.221 643 276 12
p	4

Table 5. Differences between experimental ('obs.'; Wyse et al. 1972; Cazzoli et al. 2006) pure rotational transitions and calculated ones ('calc.') for three potential energy curves PEC-X, $X = A$, S or R. All transitions have $\Delta v = 0$ and $J'' = J' + 1$. Energies are in cm^{-1}.

v	J'	obs.	(obs. − calc.) × 10^5		
			A	S	R
		$P^{14}N$			
0	0	1.567 427	−295.5	10.9	−0.5
0	1	3.134 828	−590.9	21.8	−1.0
0	2	4.702 176	−886.5	32.6	−1.6
0	3	6.269 446	−1182.0	43.5	−2.2
0	4	7.836 611	−1477.6	54.3	−2.7
0	5	9.403 643	−1773.5	65.0	−3.5
0	6	10.970 523	−2069.0	76.1	−3.8
0	7	12.537 217	−2364.8	86.9	−4.4
0	10	17.235 939	−3252.9	119.4	−6.0
0	11	18.801 641	−3549.0	130.4	−6.4
0	12	20.367 025	−3845.6	141.1	−7.2
0	13	21.932 071	−4142.2	151.9	−7.7
0	14	23.496 750	−4439.0	162.7	−8.3
0	15	25.061 036	−4736.0	173.3	−9.0
0	16	26.624 905	−5033.1	184.2	−9.5
1	1	3.112 628	−606.1	21.6	−4.7
1	2	4.668 876	−909.3	32.3	−7.1
1	3	6.225 046	−1212.3	43.2	−9.4
1	4	7.781 110	−1515.6	53.9	−11.8
1	5	9.337 046	−1818.6	64.9	−13.9
1	6	10.892 821	−2122.0	75.6	−16.4
2	2	4.635 485	−932.7	31.7	−7.9
2	3	6.180 523	−1243.8	42.2	−10.6
2	4	7.725 463	−1554.2	53.4	−12.5
3	3	6.135 871	−1276.5	40.3	−6.1
3	4	7.669 644	−1595.4	50.7	−7.4
4	3	6.091 073	−1310.7	37.2	2.6
		$P^{15}N$			
0	1	2.991 601	−561.6	22.9	1.1
0	2	4.487 339	−842.8	34.0	1.4
0	7	11.964 490	−2248.2	90.6	3.6
0	8	13.459 445	−2529.4	102.0	4.2
0	10	16.448 686	−3092.3	124.7	5.2
0	11	17.942 926	−3373.8	136.1	5.7
0	12	19.436 878	−3655.7	147.2	6.0
0	13	20.930 522	−3937.6	158.6	6.5
0	14	22.423 832	−4219.6	169.8	7.0

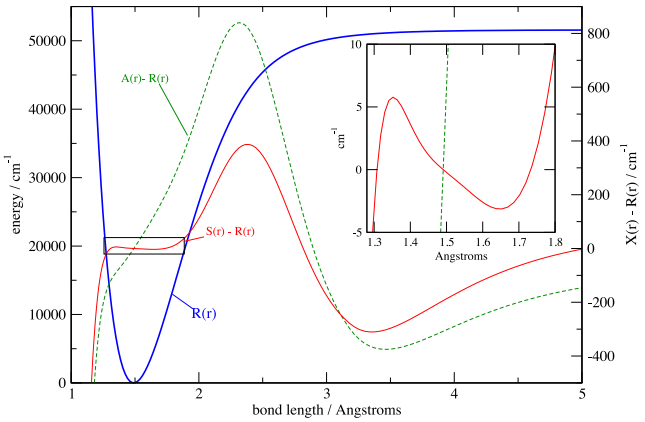

Figure 1. The thick, blue curve is the eight-parameter empirical potential PEC-R defined by equation (5) and Table 4 (vertical scale given by the axis on the left-hand side). The dashed, green curve is the difference between the ab initio PEC-A and PEC-R, and the thin, red curve the difference between the one-parameter semi-empirical PEC-S and PEC-R (vertical scale given by the axis on the right-hand side). The inset on the right is a blow-up of the area $r = 1.28$–1.80 Å contained in the black rectangle, corresponding to the range characterized by the available experimental data, while within this range PEC-S and PEC-R agree within about 10 cm^{-1}, outside this range, differences can be as large as 400 cm^{-1}.

Overall, the empirical PEC-R reproduces the experimental transition wavenumbers used in the fit (excluding the $v > 4$ simulated transitions) with an rms error of 0.004 cm^{-1}.

Fig. 1 compares the refined PEC-R with the ab initio PEC-A and the one-parameter semi-empirical PEC-S. Due to the lack of experimental data for energies higher than about 14 500 cm^{-1}, only the range $r \approx 1.28$–1.80 Å of the empirical PEC-R is well characterized. As one can see from Fig. 1, while within this range PEC-R and PEC-S agree to about 10 cm^{-1}, outside it, the two PECs differ by up to about 400 cm^{-1}. In particular, the peak visible for both PEC-A and PEC-S at $r \approx 2.30$ Å corresponds to the minimum of the c_0 curve (coefficient of the CASSCF wavefunction in the MRCI expansion, see discussion in Section 3.1). A more detailed study of the electronic structure of PN at long bond lengths would be needed to ascertain whether this feature has a physical origin or is an artefact of our calculation method, but this is beyond the scope of this work. We can however note that the difference in $J = 0$ energy levels between PEC-S and PEC-R for $v > 11$ grows approximately as $0.22 \times (v - 11)^2$ cm^{-1} up to $v = 47$ (PEC-R energy levels are the higher ones) and reaches the maximum value of 210 cm^{-1} for that value of v.

Despite this large difference in energy levels, transition frequencies with $\Delta v = 1$ (the strongest) and $v > 11$ show maximum deviations between PEC-R and PEC-S of only up to 10 cm^{-1}.

3.4 Dipole moment curve (DMC)

There appears to be no full DMC for the ground electronic state of PN available in the literature. Furthermore, there are no experimental absolute transition intensities, so it is difficult to judge the accuracy of a DMC. We therefore used the highest level of ab initio theory considered in this work, MRCI+Q/aug-cc-pCV6Z, to compute a new DMC. Dipoles were computed as the derivative of the MRCI+Q energy with respect to an external electric field along the internuclear axis for vanishing field strength (Lodi & Tennyson 2010); we used field strengths $\pm 5 \times 10^{-4}$ au and computed dipoles

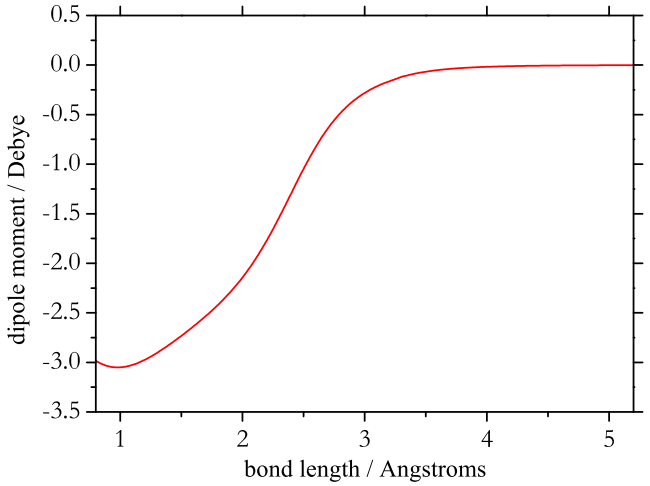

Figure 2. The ab initio MRCI+Q/aug-cc-pCV6Z DMC of PN.

Table 6. Summary of our line lists.

	$^{31}P^{14}N$	$^{31}P^{15}N$
Max v	66	68
Max J	357	366
Max ν (cm^{-1})	51 928.7	51 937.0
Number of lines	692 019	743 114
Number of energies	13 949	14 623

on a grid r = 2.1–6.1 a_0 in steps of 0.05 a_0. The corresponding DMC is shown in Fig. 2. This DMC has an equilibrium value of 2.739 D, which is close to the value of the dipole moment, 2.7465 ± 0.0006 D, determined experimentally by Raymonda & Klemperer (1971).

3.5 Computing the line list

The empirical PEC and the ab initio DMC described above were used to generate the line lists for $^{31}P^{14}N$ and $^{31}P^{15}N$ with LEVEL 8.0. The integration range was chosen as r = [1.0, 10.0] Å and the grid comprised 45 000 points. We estimated the numerical error in computed energy levels to be less than 0.0005 cm^{-1}. Table 6 summarizes the results, showing the maximal values of v, J as well as the wavenumber range considered in this work, which is far more extensive than any previous study. However, as discussed in Section 3.3, our empirical potential curve is not well characterized for energies higher than about 14 500 cm^{-1}, and therefore transition frequencies involving energy levels with energies higher than ≈14 500 cm^{-1} may have large errors of up to a few hundreds of cm^{-1}.

Following Tennyson, Hill & Yurchenko (2013), our line lists consist of an 'energy' and a 'transition' file, extracts from

Table 8. Tabulations of the partition function for $^{31}P^{14}N$ at given temperatures in kelvin compared to the values by Irwin (1981). The latter were scaled by the g_{ns} = 4 factor. The full table can be found in the supplementary material.

T	This work	Irwin (1981)
100	356.2	515.6
200	711.2	848.3
300	1068.2	1156.7
400	1434.1	1487.1
500	1817.9	1848.6
600	2227.0	2244.5
700	2666.1	2676.0
800	3138.3	3143.9
900	3645.3	3648.7
1000	4188.4	4190.8
1500	7468.0	7470.7
2000	11 717.8	11 719.8
2500	16 964.4	16 961.2
3000	23 229.7	23 215.1
3500	30 535.8	30 500.1
4000	38 905.7	38 834.1
4500	48 363.9	48 234.7
5000	58 936.7	58 719.8

Table 7. Sample extracts from the energy and transition files for $^{31}P^{14}N$. The energy files contain 13 949 entries for $^{31}P^{14}N$ and 14 623 for $^{31}P^{15}N$, while the transition files contain 692 019 entries for $^{31}P^{14}N$ and 743 114 for $^{31}P^{15}N$.

Energy file					Transition file		
N	$\tilde{E}$	g	J	v	I	F	A_{if}
1	0.000 000	4	0	0	2	1	3.0148E−06
2	1.567 437	12	1	0	3	2	2.8941E−05
3	4.702 269	20	2	0	4	3	1.0465E−04
4	9.404 461	28	3	0	5	4	2.5722E−04
5	15.673 929	36	4	0	6	5	5.1376E−04
6	23.510 567	44	5	0	7	6	9.0135E−04
7	32.914 245	52	6	0	8	7	1.4470E−03
8	43.884 806	60	7	0	9	8	2.1778E−03
9	56.422 067	68	8	0	10	9	3.1207E−03
10	70.525 819	76	9	0	11	10	4.3027E−03
11	86.195 825	84	10	0	12	11	5.7506E−03
12	103.431 825	92	11	0	13	12	7.4913E−03

N: state counting number.
$\tilde{E}$: state energy in cm^{-1}.
g: state degeneracy.
J: state rotational quantum number.
v: state vibrational quantum number.

I: upper state counting number.
F: lower state counting number.
A_{if}: Einstein $\mathcal{A}$ coefficient in s^{-1}.

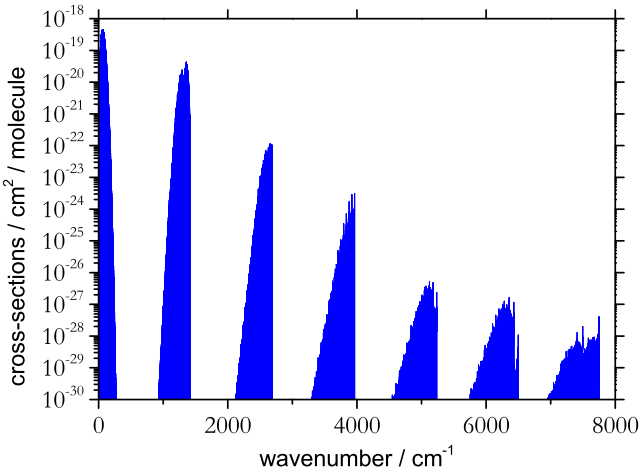

Figure 3. Overview of the absorption spectrum of ^{31}P^{14}N at a temperature of 1200 K.

which are given in Table 7. The full line list can be downloaded from the Exomol website www.exomol.com or from the VizieR service from the website of the Strasbourg astronomical Data Center (via ftp://cdsarc.u-strasbg.fr/pub/cats/J/MNRAS/ or http://cdsarc.u-strasbg.fr/viz-bin/qcat?J/MNRAS/). A small computer program which uses these files to compute spectra is given in the supplementary material.

3.6 Partition function

The partition functions, $Q(T)$, for ^{31}P^{14}N and ^{31}P^{15}N were calculated by direct summation over the energy levels using

$$Q(T) = g_{\rm ns} \sum_{i=0}^{n} (2J_i + 1)\, {\rm e}^{-E_i/(k_{\rm B}T)}, \quad (6)$$

where J_i is the rotational angular momentum quantum number and E_i is the energy of the of state i. Partition functions can be used to compute a variety of thermodynamic data.

ExoMol follows the HITRAN (HIgh Resolution TRANsmission) convention of explicitly including the full atomic nuclear spin in the molecular partition function (Fischer et al. 2003). In our case, $g_{\rm ns} = 4$ for ^{31}P^{14}N and 6 for ^{31}P^{15}N.

The ^{31}P^{14}N partition function is illustrated in Table 8, where it is compared to the values obtained from the parameters provided by Irwin (1981). The agreement is good especially considering a rather limited level of accuracy of the model used by Irwin (1981). At lower temperatures, our values do deviate somewhat from those derived by Irwin (1981), which is expected since the latter is only designed for $T > 1000$ K. In total, we have considered temperatures from 10 to 5000 K in this work, and a full table of values for the partition function values on a fine grid for the two isotopologues can be found in the supplementary material. We also computed partition functions using energy levels obtained from the semi-empirical PEC-S to estimate the error in our computed $Q(T)$. The conclusion is that our partition functions should have a relative error

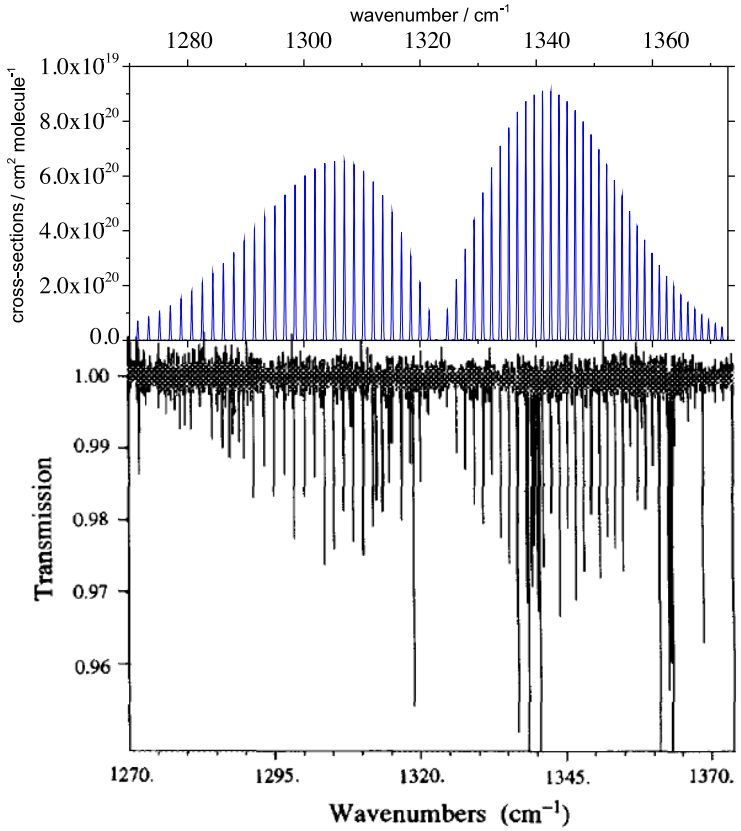

Figure 4. Comparison between the experimental spectrum of ^{31}P^{14}N by Ahmad & Hamilton (1995) and this work, at room temperature. Our work is given in the upper panel and has intensities in absolute units. The experimental data are given as a transmission spectrum and show many strong features due to water. [Reprinted from Ahmad & Hamilton (1995). Copyright 1995, with permission from Elsevier.]

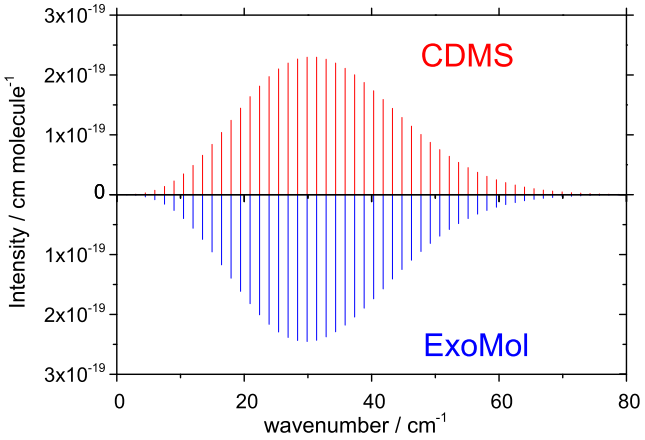

Figure 5. Comparison between the room-temperature $^{31}P^{14}N$ microwave spectrum from the CDMS (Müller et al. 2005) and this work.

of less than 0.01 per cent, i.e. they are correct to four significant digits.

3.7 Examples of ro-vibrational spectra

We used the new line list of $^{31}P^{14}N$ to compute a number of absorption spectra in the form of integrated cross-sections as described by Hill, Yurchenko & Tennyson (2013). Fig. 3 shows the absorption spectrum of $^{31}P^{14}N$ at $T = 1200$ K. Only $^{31}P^{14}N$ is presented as the difference with spectra for $^{31}P^{15}N$ can only be distinguished at high resolution. Fig. 4 compares a spectrum of $^{31}P^{14}N$ recorded by Ahmad & Hamilton (1995) with the spectrum from this work. Due to pollution of the experimental spectrum with water lines, the spectra are far from being identical; however, they show similar structures, with the P and R branches clearly visible in both spectra. This demonstrates the accuracy of our results. Another illustration is presented in Fig. 5, where the microwave spectrum of $^{31}P^{14}N$ collected in the Cologne Database for Molecular Spectroscopy (CDMS; Müller et al. 2005) is compared to our spectrum. The agreement is excellent.

4 DISCUSSION AND CONCLUSION

We produced three new PECs for PN: an ab initio PEC-A, a one-parameter semi-empirical PEC-S and a fully empirical eight-parameter PEC-R. The produced PECs are applicable to both the $^{31}P^{14}N$ and $^{31}P^{15}N$ isotopologues. The empirical PEC-R reproduces all known $^{31}P^{14}N$ experimental data up to $v = 4$ with a typical error of less than 0.01 cm^{-1} and is expected to be the most accurate of the three. Transition frequencies for the minor isotopologue $^{31}P^{15}N$ are expected to be somewhat less accurate. Experimental pure rotational transitions for both isotopologues with $v \leq 4$ (Ahmad & Hamilton 1995; Cazzoli et al. 2006) in the microwave region are reproduced within 10^{-4} cm^{-1}. Levels with $v = 5$–11 are expected to have larger errors, in the range 0.1–1.0 cm^{-1}. The accuracy of semi-empirical PEC-S should be in most cases not much worse than the quoted values for PEC-R. Errors in the ab initio PEC-A are larger by a factor of 10–100. Levels with $v > 11$ are expected to have very large errors for all PECs, in the range 10–200 cm^{-1}; however, transition frequencies with $v > 11$ and $\Delta v = 1$ should be accurate to $\approx$5 cm^{-1}. Further experimental and theoretical studies are needed to improve the accuracy for high v's.

An ab initio dipole moment was produced and, together with the PEC-R, used to compute line lists (comprising transition line positions and Einstein coefficients) for $^{31}P^{14}N$ and $^{31}P^{15}N$. Details of the line lists are reported in Table 6. The line lists cover all ro-vibrational levels up to dissociation but, as discussed above, transitions involving $v > 11$ may be seriously in error.

Partition functions accurate to about 0.01 per cent were also calculated for a range of temperatures for both isotopologues. Work done previously by Irwin (1981) shows agreement with our partition function, with the exception of temperatures below 1000 K where Irwin's results are not valid.

ACKNOWLEDGEMENT

This work is supported by ERC Advanced Investigator Project 267219.

REFERENCES

Ahmad I. K., Hamilton P. A., 1995, J. Mol. Spectrosc., 169, 286
Bartlett R. J., Musiał M., 2007, Rev. Mod. Phys., 79, 291
Barton E. J., Yurchenko S. N., Tennyson J., 2013, MNRAS, 434, 1469
Barton E. J., Chiu C., Golpayegani S., Yurchenko S. N., Tennyson J., Frohman D. J., Bernath P. F., 2014, MNRAS, 442, 1821
Bernath P. F., 2005, Spectra of Atoms and Molecules, 2nd edn. Oxford Univ. Press, Oxford
Cazzoli G., Cludi L., Puzzarini C., 2006, J. Mol. Struct. (THEOCHEM), 780, 260
Coquart B., Prudhomme J. C., 1980, J. Phys. B: At. Mol. Opt. Phys., 13, 2251
Coquart B., Prudhomme J. C., 1981, J. Mol. Spectrosc., 87, 75
Curry J., Herzberg L., Herzberg G., 1933a, J. Chem. Phys., 1, 749
Curry J., Herzberg L., Herzberg G., 1933b, Z. Phys., 86, 348
de Brouckere G., Feller D., Koot J. J. A., 1993, J. Phys. B: At. Mol. Opt. Phys., 26, 1915
Dunning T. H., 1989, J. Chem. Phys., 90, 1007
Feller D., Peterson K. A., 2013, J. Chem. Phys., 139, 084110
Fischer J., Gamache R. R., Goldman A., Rothman L. S., Perrin A., 2003, J. Quant. Spectrosc. Radiat. Transfer, 82, 401
Ghosh S. N., Verma R. D., VanderLinde J., 1981, Can. J. Phys., 59, 1640
Gingeric K. A., 1969, J. Phys. Chem., 73, 2734
Grein F., Kapur A., 1983, J. Mol. Spectrosc., 99, 25
Hill C., Yurchenko S. N., Tennyson J., 2013, Icarus, 226, 1673
Hoeft J., Tiemann E., Törring T., 1972, Z. Nat. forsch. A, 27, 703
Irikura K. K., 2007, J. Phys. Chem. Ref. Data, 36, 389
Irwin A. W., 1981, ApJS, 45, 621
Kemeny A. E., Francisco J. S., Dixon D. A., Feller D., 2003, J. Chem. Phys., 118, 8290
Le Floch A. C., Melen F., Dubois I., Bredohl H., 1996, J. Mol. Spectrosc., 176, 75
Le Roy R. J., 2006, Chemical Physics Research Report CP-662R, DPotFit 1.1 A Computer Program for Fitting Diatomic Molecule Spectral Data to Potential Energy Functions. Univ. Waterloo, Waterloo, available at: http://leroy.uwaterloo.ca/programs/
Le Roy R. J., 2007, Chemical Physics Research Report CP-663, LEVEL 8.0 A Computer Program for Solving the Radial Schrödinger Equation for Bound and Quasibound Levels. Univ. Waterloo, Waterloo, available at: http://leroy.uwaterloo.ca/programs/
Lodi L., Tennyson J., 2010, J. Phys. B: At. Mol. Opt. Phys., 43, 133001
Lodi L., Tennyson J., Polyansky O. L., 2011, J. Chem. Phys., 135, 034113
Lynas-Gray A. E., Miller S., Tennyson J., 1995, J. Mol. Spectrosc., 169, 458
Maki A. G., Lovas F. J., 1981, J. Mol. Spectrosc., 85, 368
McLean A. D., Liu B., Chandler G. S., 1992, J. Phys. Chem., 97, 8459
Milam S. N., Halfen D. T., Tenenbaum E. D., Apponi A. J., Woolf N. J., Ziurys L. M., 2008, ApJ, 684, 618

Müller H. S. P., Schlöder F., Stutzki J., Winnewisser G., 2005, J. Mol. Struct., 742, 215
Patrascu A. T., Tennyson J., Yurchenko S. N., 2014, MNRAS, submitted
Peterson K. A., Dunning T. H., 2002, J. Chem. Phys., 117, 10548
Pfeiffer B., Venkataramaniah K., Czok U., Scheidenberger C., 2012, At. Data Nucl. Data Tables, 100, 403
Raymonda J., Klemperer W., 1971, J. Chem. Phys., 55, 232
Saraswathy P., Krishnamurty G., 1987, Pramana, 29, 53
Šurkus A. A., Rakauskas R. J., Bolotin A. B., 1984, Chem. Phys. Lett., 105, 291
Szalay P., Müller T., Gidofalvi G., Lischka H., Shepard R., 2012, Chem. Rev., 112, 108
Tennyson J., 2014, J. Mol. Spectrosc., 296, 1
Tennyson J., Yurchenko S. N., 2012, MNRAS, 425, 21
Tennyson J., Hill C., Yurchenko S. N., 2013, in Gillaspy J. D., Wiese W. L., Podpaly Y. A., eds, AIP Conf. Proc. Vol. 1545, Eighth International Conference on Atomic and Molecular Data and Their Applications: ICAMDATA-2012. Am. Inst. Phys., New York, p. 186
Turner B. E., Bally J., 1987, ApJ, 321, L75
Turner B. E., Tsuji T., Bally J., Guelin M., Cernicharo J., 1990, ApJ, 365, 569
Verma R. D., Ghosh S. N., Iqbal Z., 1987, J. Phys. B. At. Mol. Opt. Phys., 20, 3961
Viana R. B., Pereira P. S. S., Macedo L. G. M., Pimentel A. S., 2009, Chem. Phys., 363, 49
Visscher C., Lodders K., Fegley B., Jr, 2006, A&A, 648, 1181
Werner H.-J., Knowles P. J., Knizia G., Manby F. R., Schütz M., 2012, WIREs Comput. Mol. Sci., 2, 242
Wong M. W., Radom L., 1990, J. Phys. Chem., 94, 638
Woon D. E., Dunning T. H., Jr, 1995, J. Chem. Phys., 103, 4572
Wyse F., Gordy W., Manson E., 1972, J. Chem. Phys., 57, 1106
Yadin B., Vaness T., Conti P., Hill C., Yurchenko S. N., Tennyson J., 2012, MNRAS, 425, 34
Yamaguchi T. et al., 2011, PASJ, 63, L37
Yamaguchi T. et al., 2012, PASJ, 64, 105
Ziurys L. M., 1987, ApJ, 321, L81

SUPPORTING INFORMATION

Additional Supporting Information may be found in the online version of this article:

Table 7. Sample extracts from the energy and transition files for $^{31}P^{14}N$ (http://mnras.oxfordjournals.org/lookup/suppl/doi:10.1093/mnras/stu1854/-/DC1)

Please note: Oxford University Press is not responsible for the content or functionality of any supporting materials supplied by the authors. Any queries (other than missing material) should be directed to the corresponding author for the paper.

This paper has been typeset from a TEX/LATEX file prepared by the author.